JACS
JOURNAL OF THE AMERICAN CHEMICAL SOCIETY

ARTICLE

pubs.acs.org/JACS

Microfluidic Synthesis of Highly Shape-Anisotropic Particles from Liquid Crystalline Elastomers with Defined Director Field Configurations

Christian Ohm,[†] Nadia Kapernaum,[‡] Dorothee Nonnenmacher,[‡] Frank Giesselmann,[‡] Christophe Serra,[§] and Rudolf Zentel*[,†]

[†]Institute of Organic Chemistry, University of Mainz, D-55128 Mainz, Germany

[‡]Institute of Physical Chemistry, University of Stuttgart, D-70569 Stuttgart, Germany

[§]LIPHT-CNRS UMR 7165, University of Strasbourg, F-67087 Strasbourg Cedex 2, France

Supporting Information

ABSTRACT: In this article, we present the synthesis of highly shape-anisotropic, micrometer-sized particles from liquid crystalline elastomers, which have the ability to reversibly change their shape in response to a certain external stimulus. For their preparation, we utilized a microfluidic setup. We succeeded in preparing sets of particles with differing degrees of shape anisotropy in their ground state including highly anisotropic fiber-like objects. All samples produced movement during the phase transition from the nematic to the isotropic phase of the liquid crystal. Depending on the direction of this shape change, we classified the samples in two groups. One type showed a contraction, while the other showed an expansion during the actuation, generating displacements of 60% and 80%, respectively. Using X-ray diffraction experiments, we could show that the different actuation properties arise from different director patterns of the liquid crystalline moieties in the microparticles. While the weakly shape-anisotropic microparticles possess a concentric director field (director perpendicular to the symmetry axis), the highly anisotropic fiber-like particles show an alignment of the director along the fiber axis. We present an explanation, claiming that this is the result of two different orientation mechanisms involving elongational flow on the one side and "log-rolling" on the other.

INTRODUCTION

Liquid crystalline elastomers (LCEs) are an interesting class of hybrid materials that combine the entropy elasticity of polymer networks (elastomers) with the ability of liquid crystals to self-organize into ordered liquid crystalline phases.[1−5] They consist of a weakly cross-linked polymer network with mesogenic moieties covalently attached to it. Two architectures are possible:[5] either the mesogens can be part of the polymer network (main-chain polymers) or they can be attached to the polymer via a flexible spacer (side-chain polymers). Within a certain temperature range, the mesogens self-organize in a liquid crystalline phase (e.g., nematic, smectic). In the case of calamitic nematics, they align with their long molecular axis parallel to each other in a common direction defining the so-called director. This mesogen alignment has a certain impact on the conformational arrangement of the polymer chains. While they exist as more or less spherical coils in an isotropic environment, the anisotropic liquid crystalline environment leads to a deformation of the individual coils. They can either stretch parallel to the director (prolate chain conformation) or perpendicular to it (oblate chain conformation) depending on the nature of the material. This coupling between the polymeric and liquid crystalline components of the hybrid material gives rise to very interesting properties. By inducing a phase transition of the mesogens between the isotropic and liquid crystalline phases, the polymer chains can be switched from a spherical to an anisotropic conformation. Consequently, LCEs are stimuli responsive polymers. Phase transitions can be triggered by various stimuli such as heat,[6−10] UV-irradiation,[11−14] electric fields,[15] or the presence of a solvent.[16] In elastomers (rubbers), in which the polymer chains are linked to each other, the macroscopic shape of the material is directly related to the conformation of the individual polymer chain. Thus, as a result of a phase transition, the transition between the two conformations will lead to a macroscopic deformation of the material. This makes LCEs interesting as materials for actuation systems.[17] The first prerequisite for an observable shape changing effect is that the polymer network must be soft enough to respond to the change of the mesogenic units. Consequently, it must be weakly cross-linked (but strong enough to prevent a flowing of the chains), and the phase transition must occur far above the network's glass transition

Received: October 22, 2010
Published: March 17, 2011

dx.doi.org/10.1021/ja1095254 | J. Am. Chem. Soc. 2011, 133, 5305–5311

temperature T_g. The second requirement for actuation is a predominantly uniform alignment of the director over the whole sample. In an untreated LCE sample, the size of one liquid crystalline domain (e.g., the area with a uniform director) is in the range of a few micrometers. If the sample is larger, many domains of different orientations exist. They induce shape changes in all directions, which compensate each other with no resulting macroscopic deformation. To prepare large LCE samples with actuation properties, the director therefore needs to be oriented uniformly. The most convenient method of producing such a sample of a so-called "liquid crystalline monodomain" is to orientate the sample just before the material is cross-linked. In this case, cross-linking permanently fixes the monodomain, and the actuation process becomes reversible. Finkelmann was the first to propose this concept and to fabricate monodomain LCEs by the addition of mesogenic molecules and cross-linking groups to polysiloxanes in a hydrosilylation reaction.[18] The reaction was performed in two steps, whereby mechanical load was applied to the sample in the second step to induce director orientation. In the following years, new materials as well as orientation techniques have been developed.[5] One of these new concepts is the application of monomeric mesogens that contain polymerizable functionalities.[19,20] These small molecule liquid crystals are easy to align and can afterward be polymerized and cross-linked radically in one step. This simple handling method allowed the preparation of structurally defined actuators on a small size scale such as pillars or cantilevers.[21−23]

In this article, we present the synthesis of oriented LCE actuators by a microfluidic process. Microfluidics offers the advantage that small objects with defined size and shape can be prepared from many different materials.[24−26] Additionally, the flowing conditions in micrometer-sized channels can also be used to induce an ordered director field orientation in liquid crystalline materials. This concept could be demonstrated in previous publications.[16,27] Now, we focus on the preparation of actuators with different shapes, ranging from spheres to disks to highly shape-anisotropic fibers. All samples showed a reversible shape change, when they were heated from the liquid crystalline to the isotropic phase. However, we found that differently shaped particles showed unlike actuation behaviors. This led to the assumption that we had prepared samples with different alignment patterns of the liquid crystalline director field. We could confirm this speculation by determining the differently shaped particle's alignment patterns in a comparative X-ray diffraction study. In the final part of this article, we present a theory, which explains the origin of the differing alignment patterns based on the flow conditions in the microfluidic setup.

SYNTHESIS OF SHAPE-ANISOTROPIC ACTUATING PARTICLES

The synthesis of shape-anisotropic particles by a microfluidic approach has been a hot topic in the last years.[28−31] The typical approach is to prepare spherical droplets from a polymerizable material by one of the microfluidic techniques[24−26] first and to force them into an anisotropic shape by flowing them through capillaries that have smaller dimensions than the droplets in one or more directions. Simultaneous photopolymerization leads to a solidification of the desired shape.

We have adapted this technique to allow the processing of liquid crystalline materials. A schematic drawing of the experimental setup is available as Supporting Information (S1). In a temperature-controlled reactor, we injected a polymerizable liquid crystalline monomer through a thin needle into a coflowing stream of silicone oil (continuous phase). This led to the formation of equally sized monomer droplets, dispersed in the continuous phase. This dispersion was tempered to the liquid crystal's nematic phase (thus allowing flow-alignment of the mesogens) and was piped through a microtube (termed "polymerization tube" in the following) with varying inner diameters. Depending on this tube's inner diameter, the droplets obtained a more or less anisotropic shape. While flowing, they were polymerized radically by UV-irradiation, locking in the desired shape as well as the mesogen alignment.

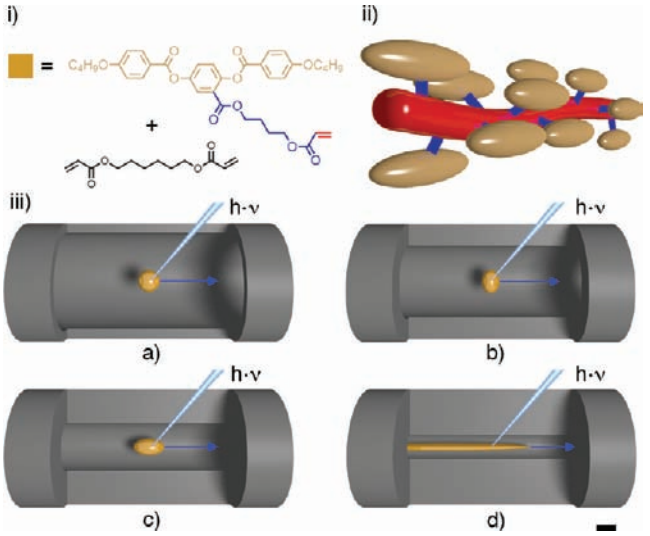

Figure 1. (i) Structure of the liquid crystalline monomer and the cross-linking agent used as a material for the preparation of particles. (ii) Schematic structure of the resulting liquid crystalline polymer. Note that the mesogens (the director) and polymer chains are parallel to each other. (iii) In-scale schematic of the polymerization of droplets from this material moving inside a microtube. The tube's inner diameter was varied between 1000 (case a) and 250 μm (case d), while the droplet diameter was kept constant at 240 μm. During polymerization, this leads to the formation of differently shaped particles resembling spheres, disks, rods, and fibers, respectively. The scale bar corresponds to 200 μm.

The chemical structure of the liquid crystalline monomer is displayed in Figure 1i. It exhibits a nematic phase at a temperature between 72 and 98 °C.[19] To achieve network formation during polymerization, we added 10 mol % of the cross-linking agent hexandioldiacrylate (Figure 1i) as a comonomer. Additionally, 2 wt % of a photoinitiator (Lucirin TPO) was added. The resulting mixture showed a monotropic nematic phase with a clearing temperature of 80 °C. The polymerization was performed at 65 °C (within the nematic phase), yielding a nematic network with a glass transition temperature of 40 °C and a transition temperature from the nematic to the isotropic phase of 130 °C. Figure 1ii shows the schematic structure of the polymer backbone. Note that the polymer chains and the director are always parallel to each other. Consequently, during the phase transition from the nematic to the isotropic phase, a contraction of the LCE material parallel to the director is expected. The viscosities of the two phases were determined by cone−plate rheology at the temperature of polymerization (65 °C). They were 0.30 Pas for the monomer mixture and 0.49 Pas for the silicone oil. The surface tension between the two

dx.doi.org/10.1021/ja1095254 |J. Am. Chem. Soc. 2011, 133, 5305–5311

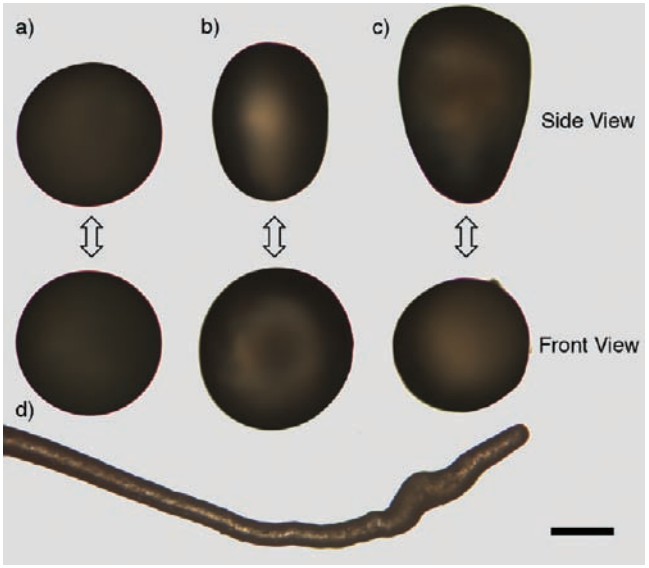

Figure 2. Microscopy images of four sets of particles polymerized inside tubes with varying diameters. Samples a—c are shown from two different perspectives. While sample a resembles a perfect sphere (front and side views are identical), the side view on sample b reveals a disk-like appearance. Sample c possesses a slightly irregular rod-shape, and sample d consists of fibers with an aspect ratio of more than 25 (the complete length of 2 mm could not be imaged). The scale bar corresponds to 100 μm.

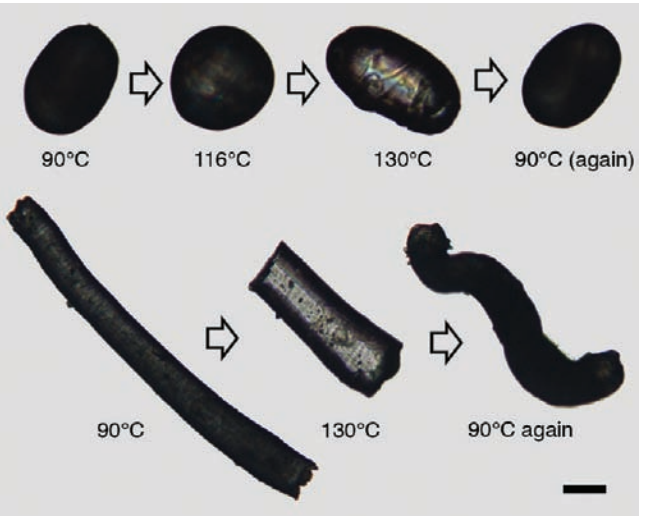

Figure 3. Shape-changing properties of two specimens of liquid crystalline elastomer particles. The samples were heated under a microscope from the nematic phase (90 °C) to the isotropic phase (130 °C) and were subsequently cooled back to 90 °C. The first row shows the actuation behavior of a disk-like particle. With increasing temperature (116 °C), it expanded perpendicular to its flat side, thereby passing through a spherical state to become rod-like. Upon cooling, it regained its disk shape. The sample in the second row was a piece from a fiber sample. In contrast to the disk, it contracted during the phase transition. When cooled back to the LC phase, it expanded to its original length, thereby curling up due to friction with the substrate. The scale bar corresponds to 100 μm.

fluids was measured by the pending drop method and was 6.25 mN/m.

Co-flowing injection was performed at a flow rate of 1.90 mL/h for the silicone oil and 0.01 mL/h for the monomer phase. This yielded droplets with a diameter of 240 μm with a very low size polydispersity (below 5%). They were polymerized in four different microtubes having inner diameters of 1.00, 0.75, 0.50, and 0.25 mm, yielding four sets of particles, termed samples a—d. An in-scale drawing of the space-situation during polymerization is given in Figure 1iii.

CHARACTERIZATION OF THE SAMPLES BY LIGHT MICROSCOPY

The first step to characterize the samples was light microscopy. To determine their three-dimensional form, the particles were imaged from two different sides. To achieve this, they were rotated on a glass slide manually with a thin needle. The microscopy images are summarized in Figure 2. We found that droplets polymerized in the tube with a diameter of 1.00 mm remained completely spherical (sample a). Sample b was polymerized in the 0.75 mm tube. The particles show one spherical and one oval side. Consequently, they must have a disk-like (oblate) shape, with an axis of symmetry perpendicular to their flat side. This shape could be confirmed by SEM measurements (see Supporting Information S2). The polymerization inside the 0.50 mm tube (sample c) yielded prolate particles with an aspect ratio of roughly 2 and low symmetry. They are rod-like but seem slightly irregularly shaped. A further reduction of the tube's inner diameter to 0.25 mm finally yielded fiber-like structures like the one shown in Figure 2d. Note that due to their length (2 mm) they could not be imaged as a whole. It should also be noted that their diameter (50 μm) is considerably smaller than the diameter of the capillary (250 μm diameter as compared to the diameter of the undeformed droplets of about 240 μm). Thus, they are not elongated by simple confinement. From the sizes determined by light microscopy, we calculated the volume of the differently shaped particles. Within the accuracy of the measurement, it was, as expected, equal for all four samples.

The trend shows clearly that decreasing the inner diameter of the polymerization tube leads to an increase of the obtained particle's shape anisotropy. This is in good agreement with work performed by Guido.[32]

He studied the shape of droplets dispersed in a continuous phase of equal viscosity while being sheared between two moving plates. They found that the amount of deformation was depending on the level of confinement (the ratio between the droplet's undeformed diameter and the gap between the plates) and the capillary number *Ca*, which defines the ratio between deforming and retracting forces. It is given by $Ca = \eta V/\gamma$, with η being the viscosity of the continuous phase, V the characteristic flow velocity, and γ the surface tension between the continuous and dispersed phases.

In our case, a decrease of the polymerization tube's inner diameter increases both the level of confinement and the capillary number (higher velocity for a given flow rate). The values for the capillary number are for sample a, $Ca = 5.4 \times 10^{-2}$; sample b, $Ca = 9.7 \times 10^{-2}$; sample c, $Ca = 2.1 \times 10^{-1}$; and sample d, $Ca = 8.7 \times 10^{-1}$. In the case of the thinnest tube (sample d, 0.25 mm diameter), the amount of shear applied on the droplets is even higher than in the work presented by Guido. This resulted in the formation of highly elongated droplets, whose shape was frozen in by the polymerization, yielding the strongly shape-anisotropic particles displayed in Figure 2.

dx.doi.org/10.1021/ja1095254 | *J. Am. Chem. Soc.* 2011, 133, 5305–5311

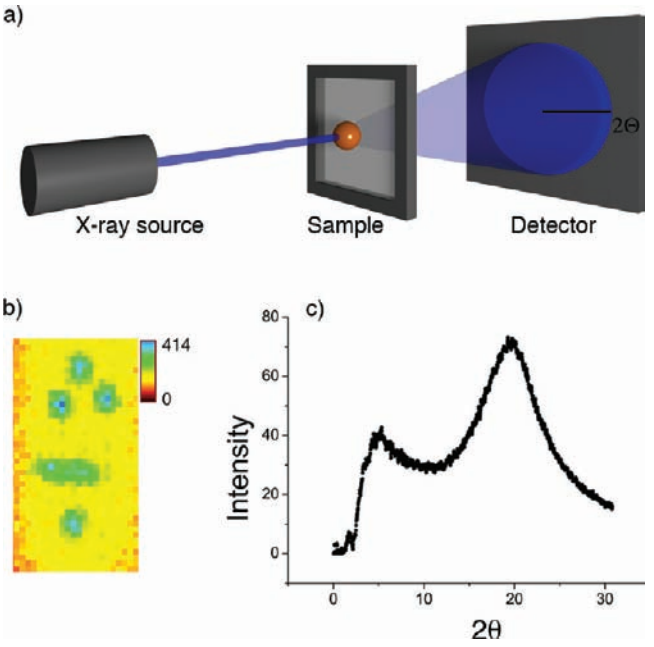

Figure 4. (a) Schematic drawing of the X-ray setup. The particles were placed on adhesive stripes attached to a sample holder and aligned manually in a specified direction. (b) To find the particles in the sample holder, X-ray absorption scans were performed by moving the holder in the *y*- and *z*-axes. The scan shows four spherical particles and one fiber. (c) The diffraction patterns of all samples showed two broad reflexes. The one at 7° corresponds to the mesogen's length, while the signal at 21° reflects the lateral distance between the mesogens.

■ ACTUATION PROPERTIES OF THE SAMPLES

In addition to their increasing amounts of shape anisotropy, the four samples exhibit different degrees of symmetry. Sample a possesses spherical symmetry. Samples b−d all have one axis of rotation perpendicular to their circular sides. However, in sample b this is the short axis (it is an oblate), and in samples c and d it is the long axis (prolate). It is a nearby consideration that these samples would show different actuation behaviors during the phase transition.

This could be confirmed by heating experiments. Single particles were dispersed in a drop of silicone oil and were heated under the microscope from 90 °C (nematic phase) to the isotropic phase (130 °C) and were afterward cooled back into the nematic phase. Thereby, all samples showed a change in shape, taking place over a temperature interval of about 20 °C. Upon cooling, the effect was reversed. The results for samples b and d are presented in Figure 3. The spheres (sample a) showed a deformation into a prolate shape, as previously reported.[27] The disks (sample b) elongated along their short axis (primal length: 190 μm), parallel to their rotational axis (Figure 3, first row). At 116 °C, they passed through a transition state where they were almost spherical before obtaining a stretched, cigar-like shape at 130 °C. In this state, the observed axis had a length of 340 μm, corresponding to an increase of 80%. During cooling, the deformation was completely reversed. The rod-like particles from sample c showed a less pronounced and slightly irregular shape change, indicating that they possessed a poor internal orientation. Finally, the fiber-like sample d showed the most spectacular deformation. The lower part of Figure 3 displays the heating experiment performed on a sample cut out from a single fiber. Unlike the disks, the fibers contracted in the direction of their rotational axis during heating. In the example shown in Figure 3, the fiber's length changed from 940 to 380 μm, which corresponds to a decrease in length of 60%. When cooled, the fiber expanded again, but curled up on the substrate. This is due to friction between the sticky material and the glass substrate. We repeated the same experiment with a shorter piece of the fiber and observed a fully reversible actuation (see Supporting Information S3).

The different actuation behaviors of the disks and the fibers indicate that the two samples possess different alignment patterns of the mesogens within their geometry. Because of the curvature and small size of the particles, the mesogens cannot be arranged in a classical monodomain, as it is observed for macroscopic samples.[8,18,33] In former publications on small droplets of liquid crystals, several possibilities to arrange a director field in a confined geometry have been described.[34−36] Examples are bipolar, axial, and concentric configurations.

■ DETERMINATION OF THE PARTICLE'S DIRECTOR ALIGNMENT BY X-RAY DIFFRACTION

A suitable method to determine the director orientation of a nematic liquid crystal is wide-angle X-ray scattering (WAXS). Aligned nematics typically show two intensity maxima in the diffuse wide angle signal orthogonal to the director.[37] This then allows the orientation of the director to be determined. Figure 4a shows a schematic drawing of the scattering experiment performed on single particles. They were placed on low-scattering adhesive stripes and were aligned in a certain direction manually under a microscope. The setup allowed a vertical and horizontal movement of the sample holder. To locate the particles, two-dimensional scans of the substrate were performed (Figure 4b) whereby they became visible as areas with increased scattering intensity. The particles were centered inside the X-ray beam, which had a diameter of 250 μm. The scattering signal was then accumulated for 60 min. Figure 4c shows the scattered intensity profile along the scattering angle 2θ. As expected for nematics, two diffuse maxima in $I(2\theta)$ were found. They correspond to the periodicities along and normal to the director, which are related to the length and the width of the mesogens.[37]

Figure 5 shows the results of three scattering experiments. It displays each scattering pattern as received by the detector, the alignment of the particles relative to the beam, and the integrated intensity $I(\chi)$ obtained by radial integration over the wide-angle arc. The first experiment (a) was performed on a disk-like particle that was placed with its side facing the X-ray beam. The diffuse wide-angle halo showed two areas of increased diffraction intensity at the meridian. Correspondingly, the plot of the integrated intensity versus the angle χ shows two maxima. In a second experiment, the particle was turned in such a way that its flat side faced the X-ray beam (b). In this case, the diffuse halo had a constant brightness. The plot of the integrated intensity versus angle χ is a flat line. The fibers were measured from the side only and showed an X-ray pattern similar to the side view of the disks with two maxima at the meridian (c).

From the maxima in the diffuse wide angle reflection, we concluded that both the disks and the fibers possess a regular orientation. However, the patterns also prove that the director field orientation of the two samples is completely different. For disk-like particles, the director is oriented in the plane of the disk, which is perpendicular to the symmetry axis (short axis of the

dx.doi.org/10.1021/ja1095254 |*J. Am. Chem. Soc.* 2011, 133, 5305–5311

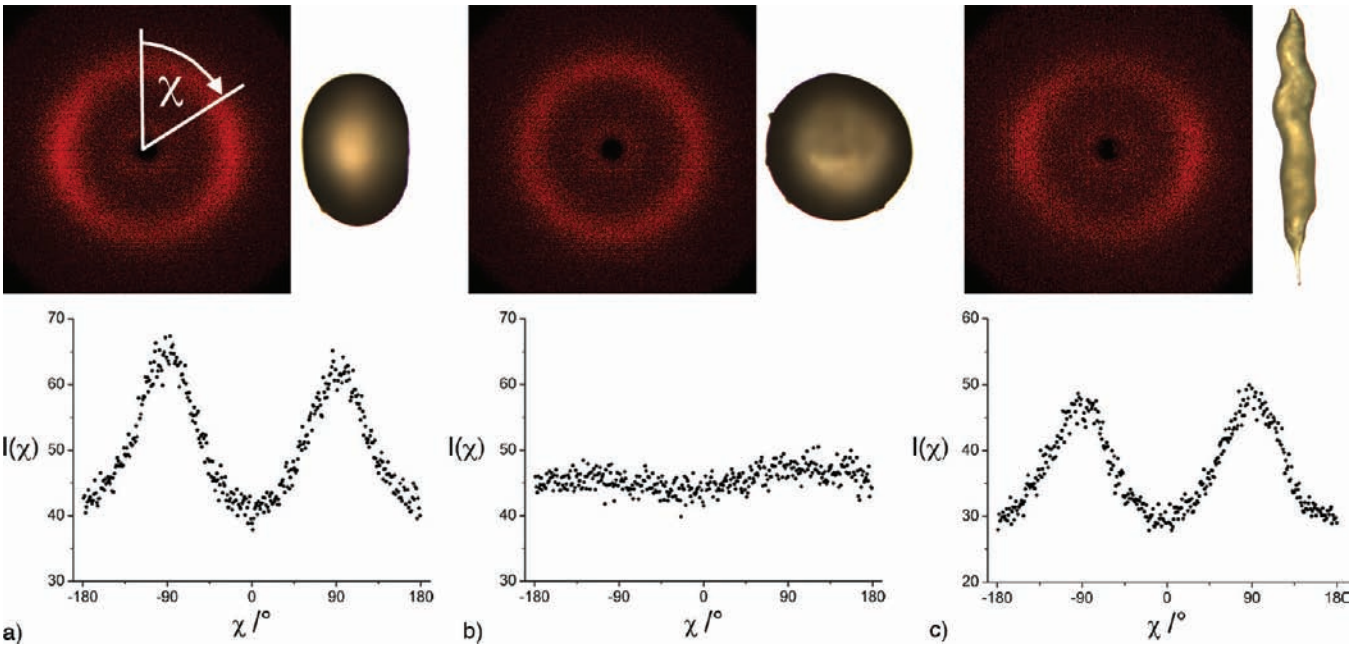

Figure 5. Results of X-ray diffraction experiments performed on a disk- and a fiber-like LCE sample. The microscope images of the samples indicate their alignment toward the X-ray beam, which runs perpendicular to the paper plane. The intensity $I(\chi)$ was obtained by radial integration over the wide-angle regime from $2\theta = 12.6°$ to 24.9°. If the X-ray beams hit the disk from the side (a), the plot showed two intensity maxima perpendicular to the particle's long axis. The same particle, measured from its flat side (b), showed a pattern with no maxima. Fibers were measured perpendicular to the beam only and thereby showed two maxima perpendicular to their long axis.

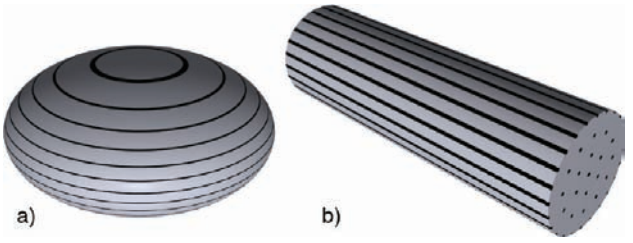

Figure 6. Schematic drawing of the director field orientation in disk- and fiber-like LCE particles. In the disks (a), the mesogens are aligned in concentric rings around the particle. These rings become smaller and smaller inside the particle, ending in a defect axis in the middle. The fibers (b) have a bipolar orientation with all mesogens aligned parallel to the fiber's long axis. This defect-free configuration leads to the drastic shape changes observed in these samples.

disk). For the fibers, the director is oriented parallel to the symmetry axis (=fiber axis). In more detail, for disks, the mesogens are aligned in concentric rings (Figure 6a). These rings become smaller inside the particle and end in a disclination axis. When scattering is performed on such a particle from the side (Figure 5a), regions with the director perpendicular to the X-ray beam (central regions) and parallel to it (side regions of the oblate object) are seen simultaneously. This leads to the superposition of an X-ray pattern with clear maxima (X-rays perpendicular to the director) and a pattern with a uniform scattering intensity (X-rays parallel to the director), and such a pattern is shown in Figure 5a. If the X-rays hit the particle from the top, the director is perpendicular to the beam, but it takes all possible orientations in the plane of the disk. This results in an equal intensity distribution over all angles χ (see Figure 5b). For the fibers, the situation is less complex. The director is aligned parallel to the fiber's axis in a bipolar arrangement (sketched in Figure 6b). This orientation leads to a selective scattering at the meridian as it was previously reported in the literature for oriented films and thicker fibers.[18,38]

As the LC-polymer used for this investigation is known to shrink parallel to the director during isotropization[10,19] (and Figure 1ii), this difference in orientation perfectly explains the difference in shape change. The fibers contract along the fiber axis, which is parallel to the director, and the disks expand parallel to their short axis, because they shrink in the plane of the disk (along the director), and so they have to expand perpendicularly to keep a constant density.

MECHANISMS OF ORIENTATION

This difference in orientation raises the question of how the "flow alignment" of the liquid crystalline material within the microfluidic device works. It seems reasonable that, depending on the flow conditions, two aligning mechanisms are possible. The first one takes place at low amounts of shear (small Ca, samples a and b) and leads to an escaped concentric alignment of the mesogens with the director perpendicular to the flow direction. The second one occurs at high shear rates (large Ca, sample d) and aligns the mesogens parallel to the flow (the fiber axis) in a bipolar fashion.

We assume that both mechanisms take place while the monomer is polymerizing, and the viscosity strongly increases. In this context, it has to be considered that the polymers subjected to the orientational processes are side-on polymers. Concerning chain anisotropy, these systems resemble LC-main chain polymers.[39,40] Consequently, they should have a similar orientation behavior. Considering this, the origin of the orientation in the fibers is straightforward. Polymerization at a high capillary number leads to

dx.doi.org/10.1021/ja1095254 |J. Am. Chem. Soc. 2011, 133, 5305–5311

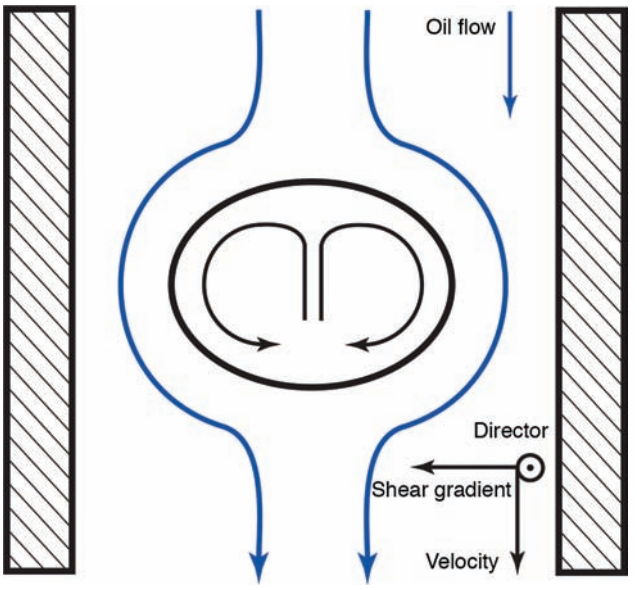

Figure 7. Schematic drawing of the "log-rolling" orientation. The liquid crystalline droplet is moving in the microtube. The oil flow induces a flow and backflow pattern within the fluid material. The velocity axis is vertical, the shear gradient is horizontal, and the vorticity axis (director) goes out of the image plane.

an elongational flow, which is generally very effective in orienting polymers and especially LC-main chain polymers parallel to the fiber axis.[41,42] It should be mentioned in this context that elongational flow is the dominant process during the spinning of fibers, which is "the method" to prepare highly oriented polymer samples. Thus, the observation that the director is parallel to the fiber axis in the LC-elastomers (sample d) is reasonable.

The origin of the concentric (or escaped concentric) configuration in the only slightly anisotropic samples (a and b) is more subtle. We assume that the flow of the continuous phase around the droplets induces stationary flow patterns inside the droplets (see Figure 7). This produces shear flow within the material. In addition, photoinduced polymerization sets in, which creates the first LC-polymers.

Besides shear alignment, shear flow can also lead to an orientation along the vortices axis as a result of "log-rolling".[43−45] That is, the director orients perpendicular to both the flow direction and the shear gradient. This orientation is especially found for small shear gradients and conditions, where entanglements are not yet very effective.[44] We speculate that these are just the conditions present in the particles at the onset of photopolymerization. Therefore, we observe "log-rolling", leading to an orientation of the director perpendicular to the flow field and thus directly to the observed concentric orientation. Later, cross-linking freezes this orientation permanently.

CONCLUSION

Systematic exploitation of these different orientation mechanisms thus allows preparing two orthogonal types of actuators from the same material in the same process. The first type shows an expansion during the phase transition, while the second one shows a contraction. This is interesting both from the point of view of fundamental science as well as for practical applications. The concept of coupling one actuator with a second one, acting in the opposite direction, is also found in natural muscles (antagonists). Combining actuators of the two types introduced in this article mimics this concept. Within a micro electro mechanical system (MEMS), such an assembly could, for example, be used to move one part of the system back and forth.

ASSOCIATED CONTENT

Supporting Information. Additional figures: S1 shows a schematic drawing of the microfluidic setup utilized to prepare the structures presented in this article. S2 shows a scanning electron microscopy photograph of a disk- or pumpkin-like particle. S3 shows an additional actuation experiment performed on a shorter part of a fiber sample. It demonstrates that the actuation is reversible in this case. This material is available free of charge via the Internet at http://pubs.acs.org.

AUTHOR INFORMATION

Corresponding Author
zentel@uni-mainz.de

ACKNOWLEDGMENT

We thank Professor Friederike Schmid for helpful discussions, the group of Professor Bernhard Wolf (WEE Solve) and Eva Fleischmann for the measurements of viscosity and surface tension, and Fay Smallwood for proofreading the manuscript. C.O. acknowledges financial support by the Graduate School of Excellence "Material Science in Mainz" (GSC 266) funded by the German Science Foundation (DFG). We also acknowledge financial support by the DFG (Ze 230/19-1).

REFERENCES

(1) Zentel, R. *Angew. Chem., Int. Ed. Engl.* **1989**, *28*, 1407–1415.
(2) Terentjev, E. M. *J. Phys.: Condens. Matter* **1999**, *11*, R239–R257.
(3) Finkelmann, H.; Brand, H. R. *Trends Polym. Sci.* **1994**, *2*, 222–226.
(4) Brand, H. R.; Pleiner, H.; Martinoty, P. *Soft Matter* **2006**, *2*, 182–189.
(5) Ohm, C.; Brehmer, M.; Zentel, R. *Adv. Mater.* **2010**, *22*, 3366–3387.
(6) Wermter, H.; Finkelmann, H. *e-Polym.* **2001**, No. 013.
(7) Sanchez-Ferrer, A.; Finkelmann, H. *Mol. Cryst. Liq. Cryst.* **2009**, *508*, 348–356.
(8) Beyer, P.; Terentjev, E. M.; Zentel, R. *Macromol. Rapid Commun.* **2007**, *28*, 1485–1490.
(9) Ahir, S. V.; Tajbakhsh, A. R.; Terentjev, E. M. *Adv. Funct. Mater.* **2006**, *16*, 556–560.
(10) Naciri, J.; Srinivasan, A.; Jeon, H.; Nikolov, N.; Keller, P.; Ratna, B. R. *Macromolecules* **2003**, *36*, 8499–8505.
(11) Yin, R. Y.; Xu, W. X.; Kondo, M.; Yen, C. C.; Mamiya, J.; Ikeda, T.; Yu, Y. L. *J. Mater. Chem.* **2009**, *19*, 3141–3143.
(12) Li, M. H.; Keller, P.; Li, B.; Wang, X. G.; Brunet, M. *Adv. Mater.* **2003**, *15*, 569–572.
(13) Finkelmann, H.; Nishikawa, E.; Pereira, G. G.; Warner, M. *Phys. Rev. Lett.* **2001**, *87*, 4.
(14) Oge, T.; Zentel, R. *Macromol. Chem. Phys.* **1996**, *197*, 1805–1813.
(15) Lehmann, W.; Skupin, H.; Tolksdorf, C.; Gebhard, E.; Zentel, R.; Kruger, P.; Losche, M.; Kremer, F. *Nature* **2001**, *410*, 447–450.
(16) Ohm, C.; Fleischmann, E.-K.; Kraus, I.; Serra, C.; Zentel, R. *Adv. Funct. Mater.* **2010**, *20*, 4314–4322.

(17) de Gennes, P. G. *C. R. Seances Acad. Sci., Ser. B* **1975**, *281*, 101–103.
(18) Kupfer, J.; Finkelmann, H. *Makromol. Chem., Rapid Commun.* **1991**, *12*, 717–726.
(19) Thomsen, D. L.; Keller, P.; Naciri, J.; Pink, R.; Jeon, H.; Shenoy, D.; Ratna, B. R. *Macromolecules* **2001**, *34*, 5868–5875.
(20) Yang, H.; Wang, L. X.; Shao, R. F.; Clark, N. A.; Ortega, J.; Etxebarria, J.; Albouy, P. A.; Walba, D. M.; Keller, P. *J. Mater. Chem.* **2009**, *19*, 7208–7215.
(21) Yang, H.; Buguin, A.; Taulemesse, J.-M.; Kaneko, K.; Bergeret, A.; Keller, P. *J. Am. Chem. Soc.* **2009**, *131*, 15000–15004.
(22) van Oosten, C. L.; Bastiaansen, C. W. M.; Broer, D. J. *Nat. Mater.* **2009**, *8*, 677–682.
(23) Yang, Z. Q.; Herd, G. A.; Clarke, S. M.; Tajbakhsh, A. R.; Terentjev, E. M.; Huck, W. T. S. *J. Am. Chem. Soc.* **2006**, *128*, 1074–1075.
(24) Il Park, J.; Saffari, A.; Kumar, S.; Gunther, A.; Kumacheva, E. . *Annual Review of Materials Research*; Annual Reviews: Palo Alto, CA, 2010; Vol. 40, pp 415−443.
(25) Serra, C. A.; Chang, Z. Q. *Chem. Eng. Technol.* **2008**, *31*, 1099–1115.
(26) Shah, R. K.; Shum, H. C.; Rowat, A. C.; Lee, D.; Agresti, J. J.; Utada, A. S.; Chu, L. Y.; Kim, J. W.; Fernandez-Nieves, A.; Martinez, C. J.; Weitz, D. A. *Mater. Today* **2008**, *11*, 18–27.
(27) Ohm, C.; Serra, C.; Zentel, R. *Adv. Mater.* **2009**, *21*, 4859–4862.
(28) Dendukuri, D.; Tsoi, K.; Hatton, T. A.; Doyle, P. S. *Langmuir* **2005**, *21*, 2113–2116.
(29) Hwang, D. K.; Dendukuri, D.; Doyle, P. S. *Lab Chip* **2008**, *8*, 1640–1647.
(30) Shum, H. C.; Abate, A. R.; Lee, D.; Studart, A. R.; Wang, B. G.; Chen, C. H.; Thiele, J.; Shah, R. K.; Krummel, A.; Weitz, D. A. *Macromol. Rapid Commun.* **2010**, *31*, 108–118.
(31) Xu, S. Q.; Nie, Z. H.; Seo, M.; Lewis, P.; Kumacheva, E.; Stone, H. A.; Garstecki, P.; Weibel, D. B.; Gitlin, I.; Whitesides, G. M. *Angew. Chem., Int. Ed.* **2005**, *44*, 724–728.
(32) Guido, S. *Curr. Opin. Colloid Interface Sci.* **2011**, *16*, 61–70.
(33) Lacey, D.; Beattie, H. N.; Mitchell, G. R.; Pople, J. A. *J. Mater. Chem.* **1998**, *8*, 53–60.
(34) Haseloh, S.; Zentel, R. *Macromol. Chem. Phys.* **2009**, *210*, 1394–1401.
(35) Haseloh, S.; van der Schoot, P.; Zentel, R. *Soft Matter* **2010**, *6*, 4112–4119.
(36) Fernandez-Nieves, A.; Link, D. R.; Marquez, M.; Weitz, D. A. *Phys. Rev. Lett.* **2007**, *98*, 4.
(37) Seddon, J. M. In *Handbook of Liquid Crystals*; Demus, D., Boodby, J., Gray, G. W., Spiess, H. W., Eds.; Wiley-VCH: Weinheim, Germany, 1998; Vol. 1: Fundamentals, pp 633−678.
(38) Li, M. H.; Keller, P.; Yang, J. Y.; Albouy, P. A. *Adv. Mater.* **2004**, *16*, 1922.
(39) Leroux, N.; Keller, P.; Achard, M. F.; Noirez, L.; Hardouin, F. *J. Phys. II* **1993**, *3*, 1289–1296.
(40) Wan, X. H.; Zhang, F.; Wu, P. Q.; Zhang, D.; Feng, X. D.; Zhou, Q. F. *Macromol. Symp.* **1995**, *96*, 207–218.
(41) Chow, A.; Keller, A.; Mueller, A. J.; Odell, J. A. *Macromolecules* **1988**, *21*, 250–256.
(42) Odell, J. A.; Keller, A.; Mueller, A. J. . *Polymers in Aqueous Media*; American Chemical Society: Washington, DC, 1989; Vol. 223, pp 193−244.
(43) Romo-Uribe, A.; Windle, A. H. *Macromolecules* **1993**, *26*, 7100–7102.
(44) Romo-Uribe, A.; Windle, A. H. *Macromolecules* **1996**, *29*, 6246–6255.
(45) Donald, A. M.; Windle, A. H.; Hanna, S. *Liquid Crystalline Polymers*; Cambridge University Press: Cambridge, U.K., 2005; Chapter 8.